Structure, Spectroscopic Study and *ab initio* Calculations on Third-order Nonlinear Optical Behavior of *N*-(2-Hydroxy-4-methoxybenzylidene)-3-nitroaniline

Hüseyin Ünver[a], Aslı Karakaş[b], Ayhan Elmalı[c], and T. Nuri Durlu[a]

[a] Department of Physics, Faculty of Sciences, Ankara University, TR-06100 Tandoğan, Ankara, Turkey

[b] Department of Physics, Faculty of Arts and Sciences, Selçuk University, TR-42049 Campus, Konya, Turkey

[c] Department of Engineering Physics, Faculty of Engineering, Ankara University, TR-06100 Tandoğan, Ankara, Turkey

Reprint requests to Dr. Hüseyin Ünver. E-mail: unver@science.ankara.edu.tr

N-(2-hydroxy-4-methoxybenzylidene)-3-nitroaniline (**1**) has been synthesized and characterized by X-ray diffraction analysis, FTIR and ^{1}H NMR spectroscopy. The maximum one-photon absorption (OPA) wavelengths recorded by quantum mechanical computations using a configuration interaction (CI) method are estimated in the UV region to be shorter than 450 nm, showing good optical transparency to the visible light. We have computed both dispersion-free (static) and also frequency-dependent (dynamic) linear polarizabilities (α) and second hyperpolarizabilities (γ) by using the time-dependent Hartree-Fock (TDHF) method to provide an insight into the microscopic third-order nonlinear optical (NLO) behavior of the title compound. The *ab initio* calculation results with non-zero values on (hyper)polarizabilities indicate that the synthesized molecule might possess microscopic third-order NLO phenomena.

Key words: Nonlinear Optical Behavior, UV/Vis Spectroscopy, FTIR, ^{1}H NMR, Hyperpolarizability

Introduction

Over the past decade, due to its applications in optical communication and processing, quadratic nonlinear optical (NLO) behavior has attracted interest of a large number of researchers in the search of materials with large microscopic and macroscopic quadratic NLO response [1]. Along with linear and quadratic effects there has been also growing interest in third-order optical nonlinearity. Organic molecules have been intensively studied with respect to their potential applications as NLO media [2 – 4]. Third-order materials have many important applications such as optical limiting and design of logic gates [5 – 6]. Actually, the third-order response governed by the second hyperpolarizability offers more varied and richer behavior than the second-order NLO process due to the higher dimensionality of the frequency space. In the light of wide applications of NLO effects, a large number of materials have been synthesized, and their NLO properties have been explored using different techniques like degenerate four-wave mixing, Z-scan and third-harmonic generation (THG). THG measurements are particularly interesting since they are strongly related to electronic processes. For free molecules, accurately determined experimental dipole and quadrupole moments and the (hyper)polarizabilities are often known and can be reproduced by *ab initio* calculations, if reasonably high correlation levels and large basis sets are used [7]. However, experimental determination of the corresponding effective properties in condensed phases is much more difficult and rests on a number of assumptions and approximations whose limitations are difficult to assess.

Schiff base compounds have been investigated during the last years because of their potential applicability in optical communication, and many of them have NLO behavior [8]. In general, Schiff base ligands consist of a variety of substituents with different electron-donating or electron-withdrawing groups, and therefore may have interesting electrochemical properties. Due to their centrosymmetric structures, non-
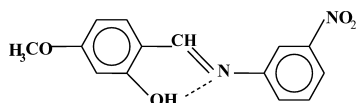
Fig. 1. Chemical structure of compound **1**.

substituted or symmetrically substituted organic compounds have been studied as third-order NLO materials. One could expect that the title Schiff base compound (Fig. 1) may show third-order NLO behavior in a centrosymmetric crystalline environment. The aim of our present study is twofold: to characterize the newly synthesized Schiff base ligand with donor-acceptor substituents with spectroscopic (UV/Vis, FTIR, ^{1}H NMR) and crystallographic (X-ray diffraction) techniques, and to investigate the third-order NLO behavior utilizing an *ab initio* time-dependent Hartree-Fock (TDHF) procedure on dispersion-free and frequency-dependent linear polarizabilities and second hyperpolarizabilities.

Results and Discussion

FTIR and ^{1}H NMR studies

The FTIR spectrum of **1** is given in the Experimental Section. The absorption band at 1624 cm^{-1} assignable to the C=N bond streching confirms the values reported in the IR spectrum of the substituted aromatic Schiff base $C_6H_7O_2CH=NC_6H_4NO_2$ [9]. The presence of the strongly electron-withdrawing NO_2 group in the compound gives rise to the highest C=N stretching frequency. The discrepancy can be ascribed to the stabilization of the C=N bond resulting from the resonance effect [10].

The ^{1}H NMR data of **1** show that the tautomeric equilibrium favors the enol form in DMSO. The Ar-O*H* proton gives a singlet at δ = 13.12 ppm. The Ar=C*H*–N and OC*H*$_3$ protons are observed at δ = 8.60 and 3.90 ppm as singlets.

Description of the crystal structure

2-Hydroxybenzaldehyde Schiff base ligands are of interest mainly due to the existence of either O–H···N or O···H–N-type hydrogen bonds and the tautomerism between enol and keto forms [11, 12]. In these types of ligands, short hydrogen bonds are observed between the 2-hydroxy group and the imine nitrogen atom. In some instances, the hydrogen atom from the phenol group is completely transferred to the imine nitrogen atom. The hydrogen bond type depends nei-

Table 1. Crystal structure data for **1**.

Formula	$C_{14}H_{12}N_2O_4$
M_r	272.26
Cryst. size, mm^3	$0.28 \times 0.26 \times 0.08$
Crystal system	triclinic
Space group	$P\bar{1}$
a, Å	7.606(2)
b, Å	8.048(3)
c, Å	10.472(3)
α, deg	82.02(3)
β, deg	79.62(3)
γ, deg	85.41(3)
V, Å^3	624.7(3)
Z	2
$D_{calcd.}$, g cm^{-3}	1.447
μ(MoK$_\alpha$), cm^{-1}	0.108
$F(000)$, e	284
hkl range	$-7 \le h \le 9, -9 \le k \le 10, -13 \le l \le 13$
$((\sin\theta)/\lambda)_{max}$, Å^{-1}	52.74
Refl. measured	4234
Refl. unique	2497
R_{int}	1042
Param. refined	184
$R(F)/wR(F^2)$ (all refls.)	0.046/0.090
GoF (F^2)	0.805
$\Delta\rho_{fin}$ (max/min), e Å^{-3}	$-0.16/0.18$
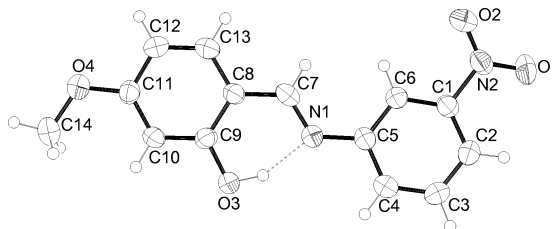
Fig. 2. The molecular structure of compound **1** in the solid state.

ther on the stereochemistry of the molecule nor on the sort of the substituent to the imine atom, but on the kind of aldehyde used. Molecule **1** contains an intramolecular O–H···N hydrogen bond [O1–H1 = 0.97 Å, H1···N1 = 1.65 Å, O1···N1 = 2.559(2) Å], which means that the compound is in the enol form as in *N*-(2-fluoro-3-methoxy)-salicylaldimine [O1–H1 = 0.87(3) Å, H1···N1 = 1.78(3) Å, O1···N1 = 2.575(2) Å] [12]. The C=N imine bond lengths and C–N–C bond angles can be compared with the values of 1.284(3) Å and 123.5(3)° in *N*-(2-fluoro-3-methoxy)-salicylaldimine [12].

Molecule **1** is not planar in the solid state (Fig. 2). The angle between the planar Schiff base moieties A (C1–C6, N1, N2, O1, O2) and B (C7–C14, O3, O4) is 4.96(8)°. The phenyl rings show small distortions from ideal geometry, and details are close to the ex-

Table 2. Selected bond lengths (Å), bond angles (deg) and torsion angles (deg) for **1**.

C1–C2	1.368(3)	C1–C6	1.375(3)
C1–N2	1.477(3)	C2–C3	1.378(3)
C3–C4	1.370(3)	C5–N1	1.409(3)
C7–N1	1.284(3)	C8–C13	1.397(3)
C9–O3	1.345(2)	C11–O4	1.362(2)
C11–C12	1.401(3)	C12–C13	1.363(3)
C14–O4	1.427(3)	N2–O2	1.221(2)
N2–O1	1.226(2)		
C4–C5–N1	116.0(2)	C1–C6–C5	118.5(2)
N1–C7–C8	122.2(2)	C9–C8–C7	120.7(2)
O3–C9–C10	117.7(2)	O3–C9–C8	121.2(2)
C10–C9–C8	121.1(2)	O4–C11–C10	124.1(2)
O4–C11–C12	114.6(2)	C7–N1–C5	123.1(2)
O2–N2–O1	123.6(2)	O2–N2–C1	118.1(2)
O1–N2–C1	118.2(2)	C9–O3–H3	103.4
C11–O4–C14	117.96(1)		
C13–C8–C9–O3	179.3(2)	C7–C8–C9–O3	−2.4(3)
C9–C10–C11–O4	−179.4(2)	O4–C11–C12–C13	178.3(2)
C4–C5–N1–C7	171.1(2)	C6–C5–N1–C7	−9.2(4)
C6–C1–N2–O1	−169.4(2)	C10–C11–O4–C14	−1.4(3)

λ_{max}	f
434.26	2.0004
402.62	1.9902
318.10	1.3031
253.31	1.1934

Table 3. Calculated maximum UV/Vis absorption wavelengths λ_{max} (nm) and oscillator strengths (f) of **1**.

pected value for aromatic rings [1.394(5) Å] [13]. The bond lengths C1–N2 = 1.447(3), N2–O1 = 1.226(2), and N2–O2 = 1.221(2) Å are within expected ranges. C–O and C=N distances are 1.345(2) and 1.284(3) Å, respectively, and are consistent with the corresponding values in similar Schiff base ligands [11, 12].

Clearly, the enol tautomer is favored over the keto form. This is evident from the observed C9–O3 bond length of 1.345(2) Å, which is consistent with a single bond, and the N1–C7 bond length of 1.284(3) Å, which is indicative of a double bond. Thus, the structure of **1** is essentially the same in the solid state and in DMSO solution. Details of the structure dermination and refinement are given in Table 1. Selected bond lengths and angles are listed in Table 2.

Computational results and discussion

The large optical nonlinearities of certain organic compounds appear to arise from extended π conjugated systems, as well as from the presence of asymmetrical charge transfer processes. Charge transfer originates from the electron-donating and electron-accepting properties of the aromatic ring substituent [14]. Dipolar molecules containing a donor and an acceptor across a π conjugation bridge have been generally recognized for large NLO response. The magnitude of the response can be easily altered by changing the donor, the acceptor or the π backbone. Quantum chemical calculations have been shown to be useful in the description of the relationship between the electronic structure of the systems and their NLO response. Actually, to accurately compute NLO properties of rather large molecular systems, there are well-tested computational codes. In particular, an accurate analysis of the NLO behavior leads to the definition of high-order hyperpolarizability values as well as third-order hyperpolarizabilities.

It can be very helpful in the investigation of NLO materials to check, apart from NLO responses, also the spectroscopic absorbance at the appropriate wavelength. Thus, the wavelengths obtained by UV/Vis spectral analysis can be helpful in planning the synthesis of promising NLO materials [15]. Since it is necessary to know the transparency region, the electronic absorption spectral studies of compounds designed to possess NLO properties are important. In this paper, the vertical transition energies and oscillator strengths from the ground state to each excited state have been computed, giving one-photon absorption (OPA), *i. e.*, the UV/Vis spectrum. The calculated wavelengths (λ_{max}) and oscillator strengths (f) for the maximum OPA of **1** are shown in Table 3. **1** has four OPA peaks in its spectrum. The optical spectra exhibit four relatively intense bands involving $\pi \rightarrow \pi^*$ transitions centered between 253 and 434 nm. The values of all absorption maxima are located in the UV region and estimated to be shorter than 450 nm, and the compunds are thus transparent in the visible region.

The hyperpolarizability tensors of molecules using a suitable computational approach can be determined. These tensors describe the response of molecules to an external electric field. Several well-established computational procedures that include electron correlation at various levels of rigor are used for the computation of NLO properties. At the molecular level, the NLO properties are determined by their dynamic hyperpolarizabilities. TDHF is a procedure generally used to find out approximate values and can be a means of understanding both static and dynamic hyperpolarizabilities of organic molecules. We present here a comprehensive *ab initio* study on the NLO properties of **1** using the TDHF method. In this study, in addition to the static linear polarizabilities $\alpha(0;0)$ and second hyperpolarizabilities $\gamma(0;0,0,0)$, the following processes for dynamic (hyper)polarizabilities have been considered:

Table 4. Selected components of the static $\alpha(0;0)$ and the $\langle\alpha\rangle(0;0)$ ($\times 10^{-24}$ esu) value of **1**.

α_{xx}	α_{yy}	α_{zz}	$\langle\alpha\rangle$
39.824	17.660	3.691	20.392

Table 5. Selected components of the frequency-dependent $\alpha(-\omega;\omega)$ and $\langle\alpha\rangle(-\omega;\omega)$ ($\times 10^{-24}$ esu) values at ω (a. u.) laser frequencies for **1**.

	$\omega = 0.05512$	$\omega = 0.04050$	$\omega = 0.04336$	$\omega = 0.02848$
α_{xx}	38.163	37.673	37.732	37.688
α_{yy}	17.819	17.673	17.697	17.606
α_{zz}	3.650	3.641	3.642	3.642
$\langle\alpha\rangle$	19.877	19.663	19.690	19.645

frequency-dependent linear polarizabilities $\alpha(-\omega;\omega)$ and THG $\gamma(-3\omega;\omega,\omega,\omega)$. Some significant calculated magnitudes of the static and frequency-dependent linear polarizabilities and second hyperpolarizabilities are shown in Tables 4 – 7, respectively.

Even π-conjugated molecules with a donor and an acceptor, lacking molecular inversion symmetry as **1**, will not display second-order NLO activity in the solid state if they crystallize in a centrosymmetric space group. Unfortunately, the title compound does crystallize in the centrosymmetric triclinic space group $P\bar{1}$ so that it does not exhibit second-order NLO properties. However, such centrosymmetric crystals might have third-order optical nonlinearity. In the Schiff bases, the valence orbitals of the nitrogen atom are sp^2 hybrid orbitals with the orbitals of the non-bonding pair of electrons being coplanar with the bonding orbital [14]. The effects of hydrogen bonds on optical properties of the crystal are important [16]. The magnitudes of static (hyper)polarizabilities are strongly enhanced by hydrogen bonds. The majority of molecular crystals with hydrogen bonding tend to enhance the NLO effects in the crystal structure [17]. Thus, the intramolecular hydrogen bond of the examined compound is likely to affect the non-zero α and γ values in Tables 4 – 7. Besides, it is expected that the introduction of a donor (-OCH$_3$)/acceptor (-NO$_2$) pair results in a larger polarization of the system in a way that increases significantly the nonlinear responses with non-zero values.

Conclusions

1 has been synthesized for the study of its third-order optical nonlinearity. Spectroscopic and crystallographic results show that the examined molecule exists in the enol form. The OPA characterization has been obtained computationally using a CI method. According to the calculation results on the linear optical be-

Table 6. All static $\gamma(0;0,0,0)$ components and the $\langle\gamma\rangle(0;0,0,0)$ ($\times 10^{-37}$ esu) value for **1**.

γ_{xxxx}	γ_{yyyy}	γ_{zzzz}	γ_{xxyy}	γ_{xxzz}	γ_{yyzz}	$\langle\gamma\rangle$
1631.940	10.163	1.106	16.183	24.618	1.341	345.499

Table 7. Selected components of the frequency-dependent $\gamma(-3\omega;\omega,\omega,\omega)$ and $\langle\gamma\rangle(-3\omega;\omega,\omega,\omega)$ ($\times 10^{-37}$ esu) values at ω (a. u.) laser frequencies calculated with the THG process for **1**.

	$\omega = 0.05512$	$\omega = 0.04050$	$\omega = 0.04336$	$\omega = 0.02848$
γ_{xxxx}	13220.403	3217.643	3744.977	2208.060
γ_{yyyy}	72.807	23.428	31.493	16.772
γ_{zzzz}	0.196	0.022	0.034	0.050
γ_{xxyy}	−114.800	37.012	33.099	38.894
γ_{xxzz}	35.546	16.282	18.054	14.625
γ_{yyzz}	2.823	1.859	1.964	1.665
$\langle\gamma\rangle$	2861.724	686.194	799.295	470.300

havior, the values of electronic transition wavelengths are estimated to be shorter than 450 nm, implying good optical transparency in the visible and near-IR region (450 – 900 nm). The computational results with non-zero values on (hyper)polarizabilities suggest that **1** might have microscopic NLO phenomena.

Experimental Section

Reagents and techniques

The ^{1}H NMR spectra were recorded on a Bruker DPX FT-NMR spectrometer operating at 400 MHz. The ^{1}H NMR chemical shifts were measured using SiMe$_4$ as an internal standard. Infrared absorption spectra were obtained from a Perkin Elmer BX II spectrometer using KBr discs, and data are reported in cm^{-1} units. The UV/Vis spectra were measured using a Shimadzu 1208 series spectrometer. Carbon, nitrogen and hydrogen analyses were performed on a LECO CHNS-932 analyzer. Melting points were measured on an Electro Thermal IA 9100 apparatus using a capillary tube. 2-Hydroxy-4-methoxybenzaldehyde, 3-nitroaniline, THF, CHCl$_3$, DMSO, ethanol, benzene and *n*-heptane were purchased from Merck (Germany).

Preparation of N-(2-hydroxy-4-methoxybenzylidene)-3-nitroaniline (**1**)

2-Hydroxy-4-methoxybenzaldehyde (5 mmol) was added to a dry THF solution (100 mL) of 3-nitroaniline (0.005 mol). The mixture was stirred and heated for 3 h. **1** was obtained after evaporation of the solvent. It was crystallized from chloroform/*n*-heptane as yellow crystals, m. p. 149 °C. – Analysis calcd. C 61.76, H 4.04, N 10.29; found C 61.82, H 3.41, N 10.18. – UV/Vis: λ_{max} (ε_{max}) = 342 nm (2556) (in C$_2$H$_5$OH); 344 nm (2156) (in THF). – IR (KBr): ν = 1570 – 1580 (Ar-NO$_2$), 1624 (C=N), 3058 – 3030

(Ar-H), 2924 – 2862 (aliph.-H), 1116 s (ArC–O), 1450 – 1600 (C=C) cm^{-1}. – ^{1}H NMR (DMSO): δ = 13.12 (s, 1 H, Ar-O*H*), 8.60 (s, 1 H, Ar=C*H*–N), 6.60 – 8.10 (m, 7 H, Ar-*H*), 3.90 (t, 3 H, OCH$_3$).

X-Ray structure determination

A suitable crystal was chosen for the crystallographic study and then mounted on a goniometer of a Stoe IPDS 2 diffractometer. All diffraction measurements were performed at r. t. (296 K) using graphite-monochromated MoK_α radiation. The collected intensities were corrected for Lorentz and polarization effects, absorption correction (μ = 0.108 mm^{-1}) was applied by the integration method using the X-RED software, and cell parameters were determined by using X-AREA software [18]. The structure was solved with Direct Methods using the WINGX implementation of SHELXS-97 [19]. The refinement was carried out by full-matrix least-squares methods on the positional and anisotropic temperature parameters of the non-hydrogen atoms. All hydrogen atoms (except H3) were positioned geometrically and refined as riding with a C–H distance of 0.93 Å. The hydrogen atom H3 was found in difference Fourier maps, calculated at the end of the refinement process as a small positive electron density, but was not refined. Other details of the data collection conditions and parameters of the refinement process are summarized in Table 1. Selected bond lengths and angles are listed in Table 2. The molecular structure with the atom numbering scheme is shown in Fig. 2 [20].

Theoretical calculations

The theoretical computations involved the determination of dispersion-free and frequency-dependent linear polarizability and second hyperpolarizability tensor components of **1** using the following methods:

The geometries of the starting structures were optimized on the *ab initio* restricted closed-shell Hartree-Fock level. The optimized structures were used to compute the linear polarizabilities and third-order hyperpolarizabilities at ω frequencies with the 6-311+G(d, p) polarized and diffused basis set. The *ab initio* TDHF method is most useful among the computational procedures to calculate (hyper)polarizabilities [21]. $\alpha(0;0)$ and $\gamma(0;0,0,0)$ at $\omega = 0$; $\alpha(-\omega;\omega)$ and $\gamma(-3\omega;\omega,\omega,\omega)$ calculations at $\omega = 0.05512$, 0.04050, 0.04336, 0.02848 atomic units (a. u.) (*i. e.* at wavelengths $\gamma = 825$, 1125, 1050, 1600 nm), often used laser frequencies in third-harmonic generation (THG) measurements, have been carried out using the TDHF method implemented in the GAMESS [22] program. In these γ definitions, the first describes the static third-order hyperpolarizabilities, the second represents the hyperpolarizability for frequency tripling, called the THG process.

In this study, the average linear polarizability $\langle\alpha\rangle$ and third-order hyperpolarizability $\langle\gamma\rangle$ values have been calculated using the following expressions [23]:

$$\langle\alpha\rangle = (\alpha_{xx} + \alpha_{yy} + \alpha_{zz})/3 \qquad (1)$$

$$\langle\gamma\rangle = [\gamma_{xxxx} + \gamma_{yyyy} + \gamma_{zzzz} + 2(\gamma_{xxyy} + \gamma_{xxzz} + \gamma_{yyzz})]/5 \quad (2)$$

Since α and γ values in the GAMESS output are reported in a. u., the calculated α and γ values have been converted into electrostatic units (esu) (1 a. u. α = 0.1482 $\cdot$ 10^{-24} esu, 1 a. u. γ = 5.0367 $\cdot$ 10^{-40} esu). To calculate all the (hyper)polarizabilities, the origin of the cartesian coordinate system (x, y, z) = (0, 0, 0) has been chosen at the center of mass of **1**.

Besides, the $\pi \rightarrow \pi^*$ transition wavelengths (λ_{max}) of the lowest lying electronic transition and the oscillator strengths (f) of these transitions for **1** have been studied theoretically by the electron excitation configuration interaction using the CIS/6-31G method in the program GAUSSIAN98W [24].

[1] M. Spassova, V. Enchev, *Chem. Phys.* **2004**, *298*, 29.

[2] A. Karakas, H. Ünver, A. Elmali, *Journal of Nonlinear Optical Physics & Materials (JNOPM)* **2007**, *16*, 91.

[3] A. Elmali, A. Karakaş, H. Ünver, *Chem. Phys.* **2005**, *309*, 251.

[4] A. Karakas, H. Ünver, A. Elmali, *J. Mol. Struct. (Theochem)* **2006**, *774*, 67.

[5] S. Shirk, R. G. S. Pong, F. J. Bartoli, A. W. Show, *Appl. Phys. Lett.* **1993**, *63*, 1880.

[6] A. Bhardwaj, P. O. Hedekvist, K. Vahala, *J. Opt. Soc. Am. B* **2001**, *18*, 657.

[7] G. Maroulis, *Chem. Phys. Lett.* **1998**, *289*, 403.

[8] M. Jalali-Heravi, A. A. Khandar, I. Sheikshoaie, *Spectrochim. Acta Part A* **2000**, *56*, 1575.

[9] H. Nazır, M. Yıldız, H. Yılmaz, M. N. Tahir, D. Ülkü, *J. Mol. Struct.* **2000**, *524*, 241.

[10] P. Nagy, R. Harzfeld, *Spect. Lett.* **1998**, *31*, 221.

[11] G. Y. Yeap, S. T. Ha, N. Ishizawa, K. Suda, P. L. Poey, W. A. K. Mahmood, *J. Mol. Struct.* **2003**, *658*, 87.

[12] H. Ünver, E. Kendi, K. Güven, T. N. Durlu, *Z. Naturforsch.* **2002**, *57b*, 687.

[13] L. E. Sutton, *Chem. Soc. Spec. Publ. Suppl.* **1965**, *18*, 516.

[14] K. Bhat, K. J. Chang, M. D. Aggarwal, W. S. Wang,

B. G. Pen, D. O. Frazier, *Mater. Chem. Phys.* **1996**, *44*, 261.

[15] J. Kulakowska, S. Kucharski, *Eur. Polymer J.* **2000**, *36*, 1805.

[16] D. Xue, S. Zhang, *J. Phys. Chem. Solids* **1996**, *57*, 1321.

[17] J. Zyss, J. F. Nicoud, M. Coquillay, *J. Chem. Phys.* **1984**, *81*, 4160.

[18] X-AREA (version 1.18) and X-RED32 (version 1.04), Stoe & Cie GmbH, Darmstadt (Germany) **2002**.

[19] G. M. Sheldrick, SHELXS-97, Program for the Solution of Crystal Structures, University of Göttingen, Göttingen (Germany) **1997**.

[20] CCDC 266594 contains the supplementary crystallographic data for this paper. These data can be obtained free of charge from The Cambridge Crystallographic Data Centre *via* www.ccdc.cam.ac.uk/data_request/cif.

[21] D. R. Kanis, M. A. Ratner, T. J. Marks, *Chem. Rev.* **1994**, *94*, 195.

[22] Intel x86 (win32, Linux, OS/2, DOS) version. PC GAMESS (version 6.2, build number 2068). This version of GAMESS is described in: M. W. Schmidt, K. K. Baldridge, J. A. Boatz, S. T. Elbert, M. S. Gordon, J. H. Jensen, S. Koseki, N. Matsunaga, K. A. Nguyen, S. J. Su, T. L. Windus, M. Dupuis, J. A. Montgomery, *J. Comput. Chem.* **1993**, *14*, 1347.

[23] M. P. Bogaard, B. J. Orr in *MTP International Review of Science*, Vol. 2, (Ed.: A. D. Buckingham), Butterworths, London, **1975**, pp. 149.

[24] M. J. Frisch, G. W. Trucks, H. B. Schlegel, G. E. Scuseria, M. A. Robb, J. R. Cheeseman, V. G. Zakrzewski, J. A. Montgomery, Jr., R. E. Stratmann, J. C. Burant, S. Dapprich, J. M. Millam, A. D. Daniels, K. N. Kudin, M. C. Strain, O. Farkas, J. Tomasi, V. Barone, M. Cossi, R. Cammi, B. Mennucci, C. Pomelli, C. Adamo, S. Clifford, J. Ochterski, G. A. Petersson, P. Y. Ayala, Q. Cui, K. Morokuma, D. K. Malick, A. D. Rabuck, K. Raghavachari, J. B. Foresman, J. Cioslowski, J. V. Ortiz, A. G. Baboul, B. B. Stefanov, G. Liu, A. Liashenko, P. Piskorz, I. Komaromi, R. Gomperts, R. L. Martin, D. J. Fox, T. Keith, M. A. Al-Laham, C. Y. Peng, A. Nanayakkara, C. Gonzalez, M. Challacombe, P. M. W. Gill, B. Johnson, W. Chen, M. W. Wong, J. L. Andres, C. Gonzalez, M. Head-Gordon, E. S. Replogle, J. A. Pople, GAUSSIAN98W (revision A.7), Gaussian Inc., Pittsburgh, PA (USA) **1998**.